J. Fluid Mech. (1980), *vol.* 96, *part* 2, *pp.* 315–334
Printed in Great Britain

Streamline patterns and eddies in low-Reynolds-number flow

By D. J. JEFFREY and J. D. SHERWOOD

Department of Applied Mathematics and Theoretical Physics,
Silver Street, Cambridge

(Received 23 February 1979)

The streamline patterns of some simple two-dimensional Stokes flows are studied and the results used both to understand and to predict the streamlines of flows in more complicated geometries, in particular the streamlines of flows that contain eddies or regions of closed streamlines. Initially, streamline patterns are studied locally, either around some special point, such as a stagnation point or a point where a streamline meets a wall, or in a special region, such as a corner. The use of these local analyses is illustrated by finding the streamlines for shear flow around a rotating cylinder; the illustration also shows how fluid in Stokes flow can be turned back on itself ('blocked'). The local analyses of flow in a corner are used to understand the eddy patterns that have been discovered in a variety of flows. The eddies occur in corner-like regions and in these regions the flow can be regarded as the superposition of two components. One component, the eddy flow, is the result of flow outside the corner stirring the fluid in the corner, while the other is the direct result of local conditions in the corner. The competition between these two components determines whether eddies actually appear in a given flow. Finally, the approach developed here is applied to a new flow situation, namely a shear flow which is bounded by a moving wall and which contains a stationary cylinder touching the wall. The streamlines deduced for different ratios of the shear strength to the wall velocity show both new eddy patterns and unexpected regions of blocked flow.

1. Introduction

For flow at very low Reynolds number, the velocity field $\mathbf{u}$ and pressure field p are governed by the Stokes equations of motion,

$$-\nabla p+\mu\nabla^2\mathbf{u}=0 \quad \text{and} \quad \nabla.\mathbf{u}=0.$$

Closed-form solutions of these equations have been found for many flow domains, and, although often these solutions have been available for some time, interest in them has not subsided. For example, the stream function for axisymmetric flow past two spheres was first derived by Stimson & Jeffery (1926), and used by them to calculate the forces acting on the spheres. There matters rested until Davis *et al.* (1976) plotted the streamlines of the flow. They found that when the gap separating the two spheres is reduced below some critical value, eddies attached to the spheres appear in the gap, filling it to an extent determined by its size. The work of Davis *et al.* was influenced by two factors which did not emerge until long after Stimson & Jeffery had published their solution. The first factor was the availability of computers which

0022–1120/80/4371–7730 $02.00

made possible numerical calculations that were too tedious for anyone of Jeffery's time to complete; the second factor was the incentive provided by the knowledge that eddies could exist in Stokes flows. Both of these factors are relevant to the present work.

Dean (1944) was the first to discover a Stokes flow which contained an eddy. The geometry he chose for his flow domain was a very special one, however, being a plane boundary that contained a projecting wall leaning over a trough, and the discovery had no air of great generality. Moffatt (1964*a*) established the idea that many solutions of the Stokes equations might contain regions of eddying flow by showing that a solution due to Dean & Montagnon (1949) for flow in a two-dimensional corner described a sequence of eddies. Moffatt did not suggest, however, that every corner region would contain eddies, something Schubert (1967) and Liu & Joseph (1977) were careful to underline, because there remained the possibility that some agency localized in the corner could affect the flow. Moffatt also observed that even for a flow which has a high Reynolds number based on its overall size, it is possible for low-Reynolds-number eddies to exist in a corner, but in fact developments of Moffatt's idea have almost all been in the context of flows with a small overall Reynolds number. In our development of Moffatt's idea, we modify his original solution with a view to understanding the intriguing eddy patterns discovered by Davis & O'Neill (1977) and Dorrepaal & O'Neill (1979).

Although determining the streamlines of a flow requires numerical computation, it need not be simply an exercise in computer programming, because often the general disposition of the streamlines is of more interest than their exact shapes, making a great deal of the computation unnecessary. Moreover, there can be large-scale features of the streamline pattern which are difficult to resolve just relying on a computer. Here streamline patterns are deduced by combining numerical calculations with a number of local analyses of the flow near certain special points or in special regions, the local analyses being based on the principles of 'matched inner and outer approximations' (Van Dyke 1975). The flow around any given point can be described by an inner approximation valid in some neighbourhood of the point and an outer approximation valid further away from the point, the inner approximation being determined partly by local conditions and partly by matching it to the outer approximation in some overlap region. Since the Stokes equations are of elliptic type, we must expect that for a general point in the flow the inner approximation will be largely determined by the matching requirement and local conditions will play only a secondary role. For a few special points, however, the local conditions will dominate the inner approximation sufficiently to allow information to be deduced which is independent, at least in its qualitative aspects, of the outer flow. For example, Moffatt's (1964*a*) eddy solution is an approximation which is valid in a special region, namely, a corner, and it provides the qualitative information that eddies can exist in a corner flow; it does not, however, provide quantitative information about the strengths of the eddies because this can come only from a matching with some particular outer flow. A note of caution on the exploitation of inner approximations has been struck by Moffatt & Duffy (1980), who have solved two problems in which inner approximations break down in ways that are quite subtle; fortunately, no such difficulties arise in the present work.

The flows studied in § 5 show the limitations of using a computer to plot stream-

lines; the unusual and complicated structures of these flows would be difficult to resolve without using the ideas developed here. Some of the results in § 2 were anticipated by Martin (1969), who had the same aim as the present one, namely supplementing numerical calculations. A physical feeling for the flow behaviour described here can be obtained by appealing to the theorem that of all flow fields satisfying a given set of boundary conditions it is the one that also obeys the Stokes equations that has the lowest rate of energy dissipation (Batchelor 1967, p. 227). This theorem applies to the flow globally and can be applied locally only with caution; nevertheless it is useful to think of regions of closed streamlines, particularly eddies, as a way of approximating a series of rigid-body rotations which are preferred because they dissipate less energy than other kinematically possible flows which require more straining.

The flow fields studied in this paper were chosen bearing two themes in mind: the presence of closed streamlines (eddies being the main special case) and the division of the flow into distinct regions, the two types of behaviour often occurring together. Looking back over earlier investigations, we can see these themes in other flows. One of the simplest flows containing closed streamlines is that produced by a point force directed perpendicular to a rigid plane (Lorentz 1896; Blake 1971; Aderogba & Blake 1978; Lighthill 1978, § 4.7). A point force in unbounded fluid produces a flow in which all streamlines are open and there is an infinite flux of fluid in the direction of the force; when a plane is present, however, the streamlines are all closed and the net flux is zero. The flow does not divide into regions. One which does is the two-dimensional flow in the annular region between two cylinders (Wannier 1950; Bentwich & Elata 1965). If the inner cylinder is sufficiently small and eccentrically placed, the flow contains two regions: one region surrounds the inner cylinder and the other clings to the outer cylinder at the widest section of the gap. As a final example, we consider the flow produced by a localized disturbance between two infinite plates (Moffatt 1964*a*; Pan & Acrivos 1967). If the flow produced by the disturbance is two-dimensional, then far from the disturbance, the flow decays by generating a sequence of eddies which extends to infinity. Thus although eddies are easiest to find in corner regions, they can fill up even infinite regions of fluid. If the flow is three-dimensional, eddies are not always found, but there do seem to be closed streamlines. Their presence in the flow is associated with a paradoxical result found by Liron (1978). He calculated the volume flux of fluid produced by a point force directed parallel to a single infinite plane. The flux is a finite quantity. If, however, the fluid is bounded by a second plane, parallel to the first, the volume flux is zero no matter how far away the second plane is from the point force and the first plane.

Two-dimensional flow fields can be described by a stream function ψ, defined in polar co-ordinates (r, θ) by

$$u_r = r^{-1}\partial\psi/\partial\theta \quad \text{and} \quad u_\theta = -\partial\psi/\partial r.$$

The stream function satisfies the biharmonic equation, which can be solved by separation of variables. The solutions for ψ and the corresponding pressure field can be put into three groups depending upon the value of a complex number λ, and they are given now for later use.

(*a*) $\lambda \neq 0, 1, 2$:

$$\psi = r^\lambda(A e^{i\lambda\theta} + B e^{i(\lambda-2)\theta}) \quad \text{and} \quad p = 4\mu(\lambda-1)r^{\lambda-2} i B e^{i(\lambda-2)\theta}, \qquad (1.1\,a, b)$$

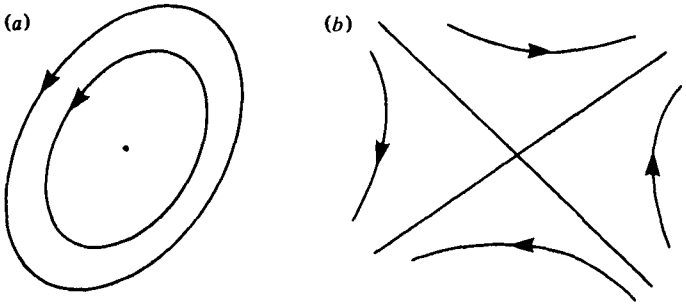

FIGURE 1. Flows near a stagnation point. (a) $|\zeta| > |e|$; (b) $|\zeta| < |e|$, the smaller angle between the stagnation-point streamlines is $\frac{1}{2}\pi - \arcsin|\zeta/e|$.

or equivalently

$$\psi = (Ar^{\lambda} + Br^{\lambda+2})\, e^{i\lambda\theta} \quad \text{and} \quad p = 4\mu(\lambda+1)\, r^{\lambda} iB e^{i\lambda\theta}.$$

(b) Special cases $\lambda = 0, 1, 2$:

$$\psi = A e^{2i\theta} + C\theta + D \quad \text{and} \quad p = 4\mu r^{-2} iA e^{2i\theta}; \tag{1.2a, b}$$

$$\psi = r(A e^{i\theta} + B\theta e^{i\theta}) \quad \text{and} \quad p = 2\mu r^{-1} B e^{i\theta},$$

or alternatively

$$\psi = (Ar + Br\log r)\, e^{i\theta} \quad \text{and} \quad p = -2\mu r^{-1} iB e^{i\theta};$$

$$\psi = r^2(A e^{2i\theta} + C\theta + D) \quad \text{and} \quad p = 4\mu C \log r. \tag{1.3a, b}$$

(c) Solution independent of θ

$$\psi = Ar^2 \log r + B\log r + Cr^2 + D \quad \text{and} \quad p = -4\mu A\theta.$$

2. Special points in the flow

The position in a flow field of a special point, such as a stagnation point, is determined by the entire flow, but by assuming that the position is known, we can use a local analysis to deduce qualitative information about the flow near the special point. We now describe those local analyses of two-dimensional flow that are relevant to the present work.

2.1. *Isolated stagnation point*

Given a stagnation point in the interior of the fluid, we can use it as the origin for polar co-ordinates (r, θ) or Cartesian co-ordinates (x, y) and write the stream function for the flow as

$$\psi = r^2(\zeta + e\sin 2\theta) = \zeta(x^2 + y^2) + 2exy,$$

where ζ and e are the vorticity and the rate of strain evaluated at the stagnation point. The possible streamline patterns are shown in figure 1. The pattern in figure 1(*a*) corresponds to an extremum in ψ and will be called a centre stagnation point, while that in figure 1(*b*) corresponds to a saddle (stagnation) point. To decide between them for some given stream function $\psi(\xi, \eta)$, we evaluate the quantity

$$\psi_{\xi\xi}\psi_{\eta\eta} - \psi_{\xi\eta}^2 = 4(\zeta^2 - e^2) \tag{2.1}$$

at the stagnation point (where $\psi_{\xi} = \psi_{\eta} = 0$). It is positive for an extremum and negative for a saddle point (Burkill 1962, § 8.8).

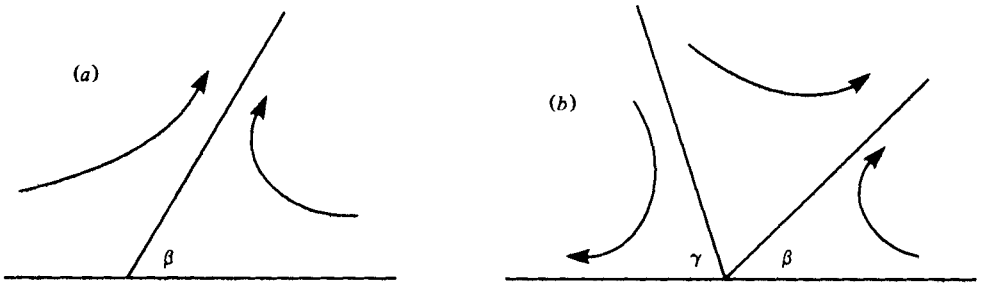

FIGURE 2. Streamlines near a point of zero tangential stress.
(a) $n = 1$, (b) $n = 2$, $\gamma = \arctan(3\cot\beta)$.

2.2. *Point of zero tangential stress on a boundary*

The point at which one or more streamlines intersect a rigid boundary is a point of zero tangential stress. The case of one streamline meeting a wall was analysed by Batchelor (1967, §4.8) and Michael & O'Neill (1977), who concluded that the streamline could meet the wall at any angle. Schubert (1968) and Dandapat & Gupta (1978) offered an alternative analysis in which they suggested that when a streamline meets a rigid wall at an angle β (figure 2*a*), the flow must be described by the general solution (1.1*a*) with the constants taking different values on either side of the dividing streamline $\theta = \beta$. They were then left with eight unknown (real) constants and the power λ to determine. They obtained an eigenvalue problem for λ by deriving eight homogeneous equations for the constants. As well as showing that λ could be any integer, they obtained for it a non-integral value which depended upon β. This last value is, however, spurious because there is a ninth equation for the eight constants, obtained by requiring that the velocity tangential to the streamline $\theta = \beta$ be continuous; this equation is independent of the other eight and makes the system over-determined unless some of the equations are satisfied trivially. If λ is an integer, the over-determinacy of the system is relieved and the constants have the same values on either side of $\theta = \beta$, but the non-integral value of λ does not achieve this. In what follows, then, we shall assume one form of solution for all values of θ.

We now turn to the case in which n streamlines meet a wall at the same point, the generalization from one streamline being prompted by a flow discussed in §5 in which two streamlines meet a wall. The stream function given by Michael & O'Neill (1977) for the local flow near a point of zero tangential stress can be written

$$\psi = Ar^{n+2}\left[\frac{\cos(n+2)\theta - \cos n\theta}{\cos(n+2)\beta - \cos n\beta} - \frac{n\sin(n+2)\theta - (n+2)\sin n\theta}{n\sin(n+2)\beta - (n+2)\sin n\beta}\right], \tag{2.2}$$

where n is an integer (determined by the outer flow) and β is the angle between one of the streamlines and the wall. In this form, (2.2) describes a 'fan' of n streamlines meeting the wall at $r = 0$, except in one special case when the number is $n-1$; we show this by counting the zeros of the term in square brackets, ignoring $\theta = 0, \pi$. The factors

$$\cos(n+2)\theta - \cos n\theta \quad \text{and} \quad n\sin(n+2)\theta - (n+2)\sin n\theta$$

have, respectively, a zero and an extremum when

$$\theta = l\pi/(n+1), \quad \text{where} \quad l = 1, 2, \ldots, n.$$

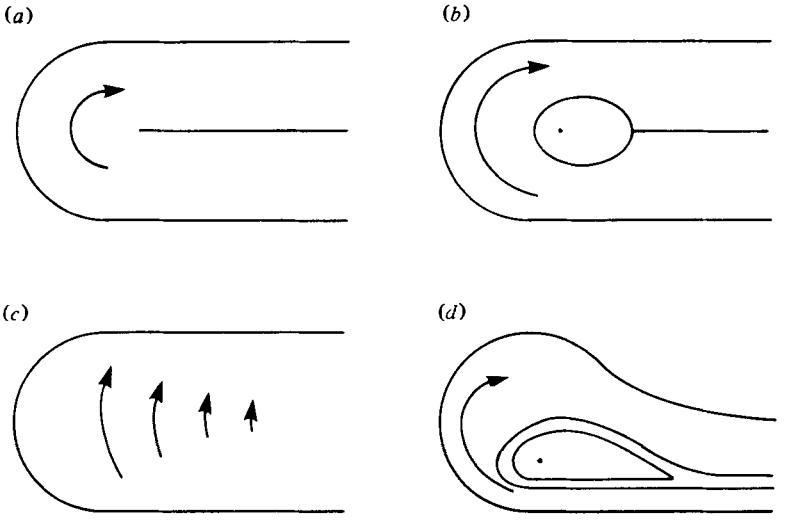

FIGURE 3. Conjectured ways in which a fluid flow might be turned back on itself.

Consecutive extrema of the second factor have opposite signs, implying that it has $n-1$ zeros. A linear combination of the two factors has n zeros except when

$$n\sin(n+2)\beta-(n+2)\sin n\beta = 0;$$

in this special case there are $n-1$ zeros and the tangential shear stress is zero everywhere on the wall, not just at $r = 0$.

The particular cases $n = 1$ and $n = 2$ are depicted in figure 2. The case $n = 2$ illustrates several points which are general. The outer flow does not determine the angles made by the two streamlines independently; if one streamline makes an angle β, the other must make an angle $\gamma = \arctan(3\cot\beta)$. Consequently, for the symmetric flow studied in § 5 we must have $\beta = \arctan(3\cot\beta) = \frac{1}{3}\pi$. The special case of $n-1$ streamlines is the limit $\beta \to 0$ and $\gamma \to \frac{1}{2}\pi$ or vice versa.

2.3. *Zero-velocity streamlines in regions of blocked flow*

Regions of 'blocked' flow, in which fluid enters from infinity, turns around and flows back in the direction it came from, are found in several of the flows studied later, and this leads us to investigate the streamline patterns associated with such behaviour. Four apparent possibilities for blocked flow are shown in figure 3. The first two are based on the fact that, in a simple shear flow, the streamline that separates fluid flowing in one direction from fluid flowing in the other is a streamline with zero velocity at all points along it; if we assume that such a streamline can persist in a 'blocking' situation, it could either simply come to an end (figure 3*a*) or intersect an eddy (figure 3*b*). If no zero-velocity streamline is present, then the turning-back motion could be similar at all points (figure 3*c*) or the fluid could circle around a region of closed streamlines, the boundaries of which asymptote together at infinity (figure 3*d*).

We now show that the first two patterns are not possible because no streamfunction can be found for local flow around the tip of a zero-velocity streamline. The method is similar to one used by Martin (1969) who showed that three streamlines could not

meet at a point. A zero-velocity streamline is equivalent to a rigid plate with the additional constraint that the stress across it must be continuous. Michael & O'Neill (1977) show that the flow around the end of a rigid plate is described by the stream function

$$\psi = r^{\frac{1}{2}m}\{A[\cos\tfrac{1}{2}m\theta - \cos(\tfrac{1}{2}m-2)\theta] + E[(\tfrac{1}{2}m-2)\sin\tfrac{1}{2}m\theta - \tfrac{1}{2}m\sin(\tfrac{1}{2}m-2)\theta]\}, \quad (2.3)$$

where $m = 3, 5, 6, 7, 8, \ldots$. The line $\theta = 0$ is the zero-velocity streamline, but if m is even the line $\theta = \pi$ is also a zero-velocity streamline (cf. last section) contradicting our assumption that we are at the tip of this streamline. Therefore m must be odd. The pressure field associated with (2.3) is

$$p = -4\mu(\tfrac{1}{2}m-1)\, r^{\frac{1}{2}m-2}[A\sin(\tfrac{1}{2}m-2)\theta - \tfrac{1}{2}mE\cos(\tfrac{1}{2}m-2)\theta].$$

Putting $\theta = 0, 2\pi$ in this expression we find that the pressure is discontinuous across $\theta = 0$ when m is odd unless $E = 0$. But setting $E = 0$ in (2.3) restricts us to flow fields which are symmetric about $\theta = 0, \pi$ and which have $\theta = \pi$ a streamline (but not a zero-velocity one). We cannot build up the flow patterns shown in figure 3(*a*) and (*b*) from these flow fields. Thus regions of blocked flow must look like figure 3(*c*) and (*d*).

3. The streamlines around a cylinder rotating in a shear flow

If a cylinder of unit radius is placed on the zero-velocity streamline of a shear flow of strength κ and rotated at an angular velocity Ω, the streamlines of the various flows obtained can be deduced without detailed numerical calculation by using the results of § 2.1; the results provide simple examples of blocked flow and regions of closed streamlines. The stream function for the flow is (Bretherton 1962)

$$\psi = -\Omega\log r + \tfrac{1}{4}\kappa[2r^2\sin^2\theta + (2-r^{-2})\cos 2\theta - 2\log r - 1] \quad (3.1a)$$

$$= \tfrac{1}{4}\kappa[2r^2\sin^2\theta + (2-r^{-2})\cos 2\theta - 2\omega\log r - 1], \quad (3.1b)$$

where $\omega = 1 + 2\Omega/\kappa$. We first find the stagnation points of the flow. In Cartesian co-ordinates $x = r\cos\theta$ and $y = r\sin\theta$ there are saddle stagnation points at

$$x = \pm\omega^{-\frac{1}{2}}, \quad y = 0$$

and

$$x = 0, \quad y = \pm\tfrac{1}{2}[\omega + (\omega^2+8)^{\frac{1}{2}}]^{\frac{1}{2}}.$$

We also need the asymptotic form far from the cylinder of the streamline $\psi = \psi_0$. Provided $\omega > 0$, it is

$$y^2 = \omega\log x - 4\psi_0/\kappa - \tfrac{1}{2} + O(y^2/x^2). \quad (3.2)$$

There are five cases to consider (cf. Robertson & Acrivos 1970).

3.1. *Cylinder rotating against shear, $\omega > 1$*

When $\omega > 1$, only the stagnation points on the y axis are in the fluid. Between the stagnation points and the cylinder, the fluid is rotating with the cylinder, while further away the streamlines are going to infinity according to the asymptotic relation (3.2). From these considerations, the streamline pattern can be drawn as shown in figure 4(*a*). Note that the region of blocked fluid is an example of the conjectured figure 3(*c*), and the region of closed streamlines is rotating against the shear flow.

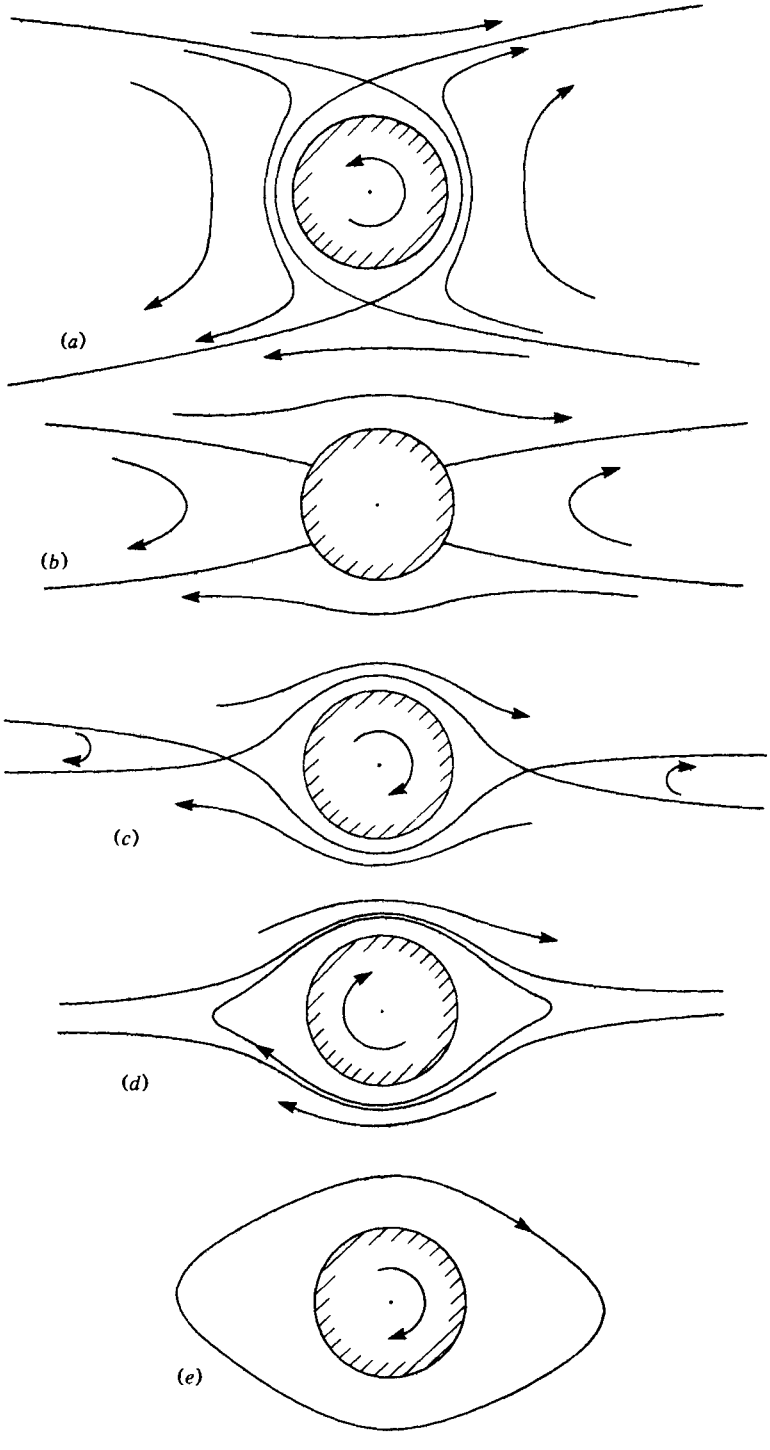

FIGURE 4. Streamlines around a rotating cylinder in shear flow. (a) $\omega > 1$, cylinder rotating against shear; (b) $\omega = 1$, cylinder stationary; (c) $0 < \omega < 1$, cylinder rotating slower than freely suspended one; (d) $\omega = 0$, freely suspended cylinder; (e) $\omega < 0$, cylinder rotating faster than a freely suspended one.

3.2. *Stationary cylinder*, $\omega = 1$

All points on the cylinder are now stagnation points. It is possible, therefore, for streamlines to meet the cylinder at points of zero tangential stress. We test for this by calculating $\partial^2\psi/\partial r^2$ on $r = 1$ and find it is zero at $\theta = \pm\frac{1}{6}\pi$. Again remembering the asymptotic form (3.2), we obtain figure 4(*b*).

3.3. *Cylinder rotating slower than a freely suspended one*, $0 < \omega < 1$

Now it is the stagnation point on the x axis which is outside the cylinder and we obtain the flow shown in figure 4(*c*). The region of closed streamlines around the cylinder is now rotating in the same sense as the vorticity of the shear flow, but more slowly.

3.4. *Freely suspended cylinder*, $\omega = 0$

This case was studied by Cox, Zia & Mason (1968); the streamlines are drawn in figure 4(*d*). There are no stagnation points in the flow and there is no region of fluid being blocked by the cylinder. The region of closed streamlines around the cylinder now extends to infinity, where its boundaries asymptote together and provide an example of the asymptotic behaviour suggested in figure 3(*d*). The transfer of heat across this flow was studied by Nir & Acrivos (1976) who found that at high Péclet number the presence of closed streamlines had an important influence on the magnitude of the heat flux.

3.5. *Cylinder rotating faster than a freely suspended one*, $\omega < 0$

All streamlines are now closed; see figure 4(*e*).

4. Eddies in corner-like regions

Two approaches have been used to study the ways in which eddies can form in Stokes flow. The first derives an inner approximation for flow in a corner region and the second analyses the complete solution of a fully-specified problem. The first approach started with Moffatt (1964*a*) and Lugt & Schwiderski (1965), who independently studied two-dimensional flow between two rigid plane walls, and it has been extended by Schwiderski, Lugt & Ugincius (1966), Wakiya (1976) and Liu & Joseph (1978), who all studied flow in a conical corner, and by Hynes (1978), who studied the flow between two conical surfaces which share a common vertex. The second approach, based on globally valid solutions, was used by Moffatt (1964*b*) to complement the local analysis of Moffatt (1964*a*). By devising a complete problem that he could solve, Moffatt showed explicitly how a globally valid solution asymptoted to the eigensolutions of his inner analysis. Of the later work that has followed this second approach, we have selected three papers for further study here: Schubert (1967), Davis & O'Neill (1977) and Dorrepaal & O'Neill (1979).

Schubert (1967) solved several problems in the two-dimensional flow of viscous fluid bounded by a cylinder touching a plane. One problem was that of shear flow over a stationary boundary; from his solution, Schubert found that the flow in the cusp between the cylinder and the plane consisted of eddies. This result suggested that Moffatt's (1964*a*) analysis might be used qualitatively to understand the flow in any corner-like region. Schubert also found the flow produced when the plane moved

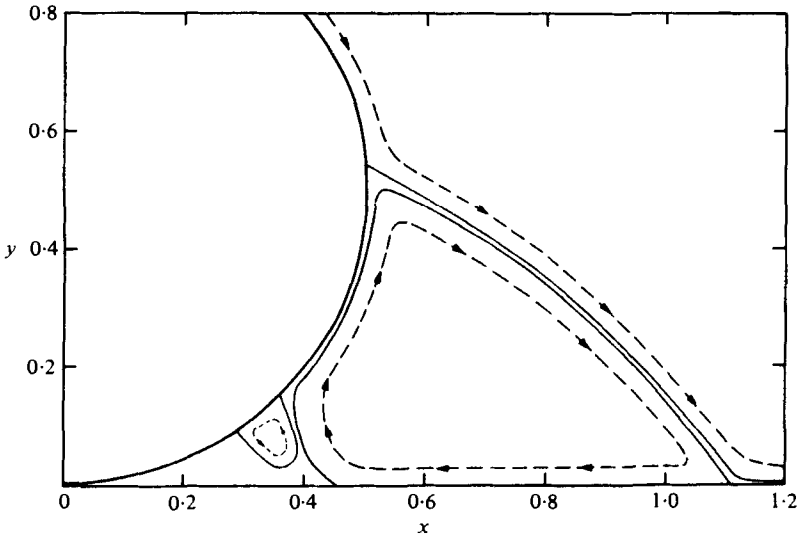

FIGURE 5. Shear flow over a cylinder which almost touches a plane (Davis & O'Neill 1977). Fluid passing under the cylinder leaves the gap region by passing around the projecting eddies.

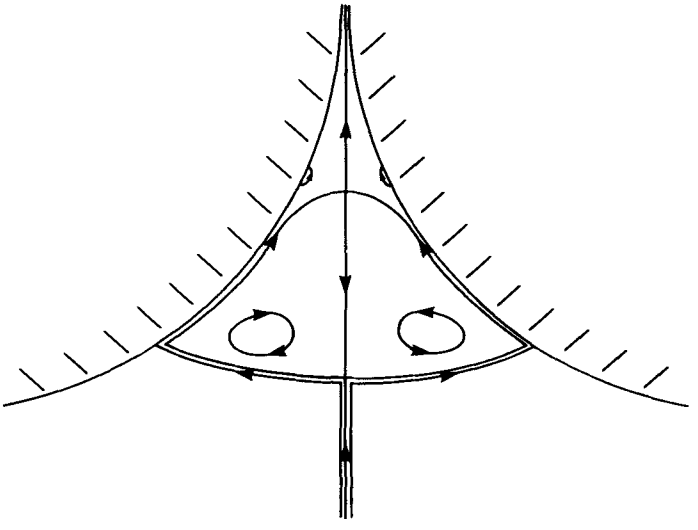

FIGURE 6. Streaming flow past two cylinders (Dorrepaal & O'Neill 1979). The eddy in the middle of the gap is not attached to a wall.

parallel to itself and the cylinder was held stationary. He pointed out that no eddies existed in this flow, making the point that Moffatt (1964*a*) had not intended to suggest that eddies form in every corner-like region in every flow. Davis & O'Neill (1977) modified Schubert's flow domain by separating the cylinder from the plane so that fluid could flow under the cylinder. They solved for the shear flow over the cylinder and plane, and discovered curious eddy patterns such as the one shown in figure 5. This pattern is interesting because the number of eddies is finite and because the route followed by the fluid emerging from the gap between the cylinder and the plane is so circuitous. Finally, Dorrepaal & O'Neill (1979) studied streaming flow past two cylinders which almost touched, and found eddy patterns such as that shown in figure 6.

The new feature of this pattern is the way in which there is a 'free' eddy in the flow not attached to any wall.

Moffatt (1964*a*) gave antisymmetric and symmetric solutions for flow between two plane walls meeting at an angle 2α. The stream function for the flow that is antisymmetric about the centre-line of the corner is

$$\psi = Ar^{\lambda}[\cos\lambda\theta\cos(\lambda-2)\alpha - \cos(\lambda-2)\theta\cos\lambda\alpha], \tag{4.1}$$

where λ is an eigenvalue satisfying $\sin 2(\lambda-1)\alpha = -(\lambda-1)\sin 2\alpha$. It is complex for $2\alpha < 146°$, which indicates that eddies are present in the flow. The stream function for the symmetric flow is

$$\psi = Br^{\nu}[\sin\nu\theta\sin(\nu-2)\alpha - \sin(\nu-2)\theta\sin\nu\alpha],$$

where ν satisfies $\sin 2(\nu-1)\alpha = +(\nu-1)\sin 2\alpha$ and is complex, again indicating eddies, for $2\alpha < 159°$ (Moffatt & Duffy 1980 have corrected the figure 156° given in Moffatt 1964*a*). The factors A and B are arbitrary scale factors which would be determined by matching with some outer flow; for our purposes they can be set to 1. The patterns corresponding to the lowest eigenvalues for λ and ν are shown in figures 7(*a*) and 8(*a*) respectively, having been plotted using a computer graphics package. The stagnation points are indicated as well as the streamlines.

The antisymmetric case helps us understand the flow in figure 5. The gap between the cylinder and the plane allows fluid to enter the corner region and therefore acts as a source. This leads us to guess that patterns similar to figure 5 can be obtained by adding to (4.1) the stream function for the flow produced by a line source at the vertex of the corner. If the source has strength Q, the new stream function is

$$\psi = r^{\lambda}[\cos\lambda\theta\cos(\lambda-2)\alpha - \cos(\lambda-2)\theta\cos\lambda\alpha] + Q\frac{2\theta\cos 2\alpha - \sin 2\theta}{2\alpha\cos 2\alpha - \sin 2\alpha}. \tag{4.2}$$

The streamlines and stagnation points for a particular value of Q are shown in figure 7(*b*) (also plotted using computer graphics). The actual numerical value of Q is not significant because it depends upon arbitrary choices of scale. As an aid to understanding the computer picture, a schematic diagram which uses distorted scales is shown in figure 7(*c*). It should be noted that eddies are absent from points of the flow sufficiently near the source and also that eddies project into the flow alternately from the upper and lower walls. The interpretation of figure 7(*b*) was verified by calculating separately the positions of the special points of § 2. The critical distance from the vertex below which no special points can be found is proportional to Q^{p}, where $p = 1/Re\{\lambda\}$. To understand this flow in a way that can be transferred to other situations, we note that the two terms in (4.2) correspond to different mechanisms. The eddy term is a result of flow outside the corner stirring the fluid in the corner and it becomes more dominant the further one is from the vertex; it is an eigensolution in the terminology of Van Dyke (1975, § 4.5). The source term is the result of a local disturbance centred on the vertex and it always dominates the eddy flow near enough to the corner; we can contrast it with the eigensolution by calling it 'locally forced'. The relative strengths of these components determine the distance from the corner at which the eddies first appear, but it should be noted that, because the corner in figure 7 is infinite, it will always be possible to find some distance at which eddies appear.

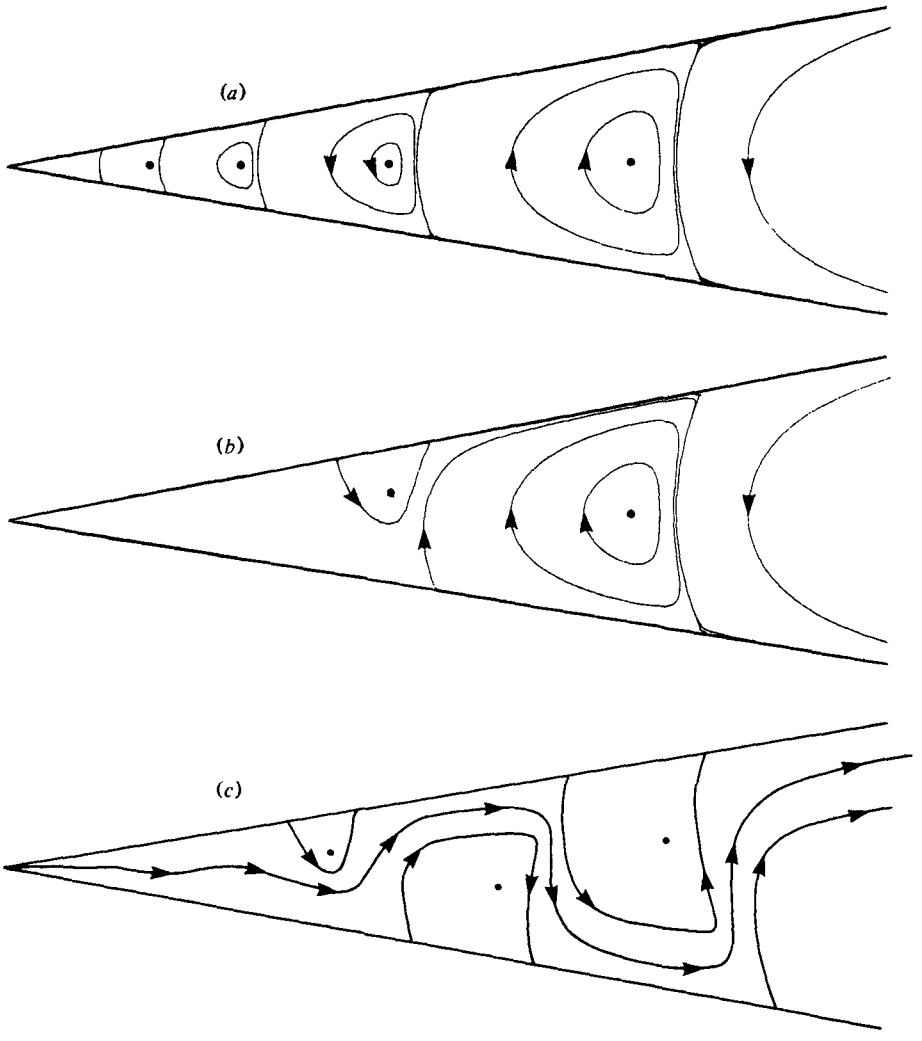

FIGURE 7. Antisymmetric eddies and a source flow for $\alpha = \frac{1}{16}\pi$ and $\lambda = 4{\cdot}216 + 2{\cdot}229i$. (a) $Q = 0$, (b) $Q = 5$, (c) Schematic picture of flow. Centre stagnation points are marked by dots.

We now relate these observations to figure 5 which contains the additional features that the number of eddies is finite (and may be zero) and the size of the corner is finite. The eddy component of the flow is driven by the fluid which must flow upwards to clear the cylinder. This stirring has a magnitude determined by the complete flow and the geometry of the flow domain, but it will be practically constant over the range of small gap widths that we are considering. On the other hand, the strength of the source (the amount of fluid flowing through the gap) is sensitive to the gap width, being proportional, asymptotically, to $h^{\frac{1}{2}}$, where h is the gap width. This can be predicted from lubrication theory for flow through a narrow passage or verified directly from the complete solution (Davis & O'Neill 1977). Thus there is a minimum distance from the gap at which eddies can appear, and this distance increases with the gap width. There is also a maximum distance at which eddies can be found. This is the distance at which the inner approximation ceases to be applicable because of the

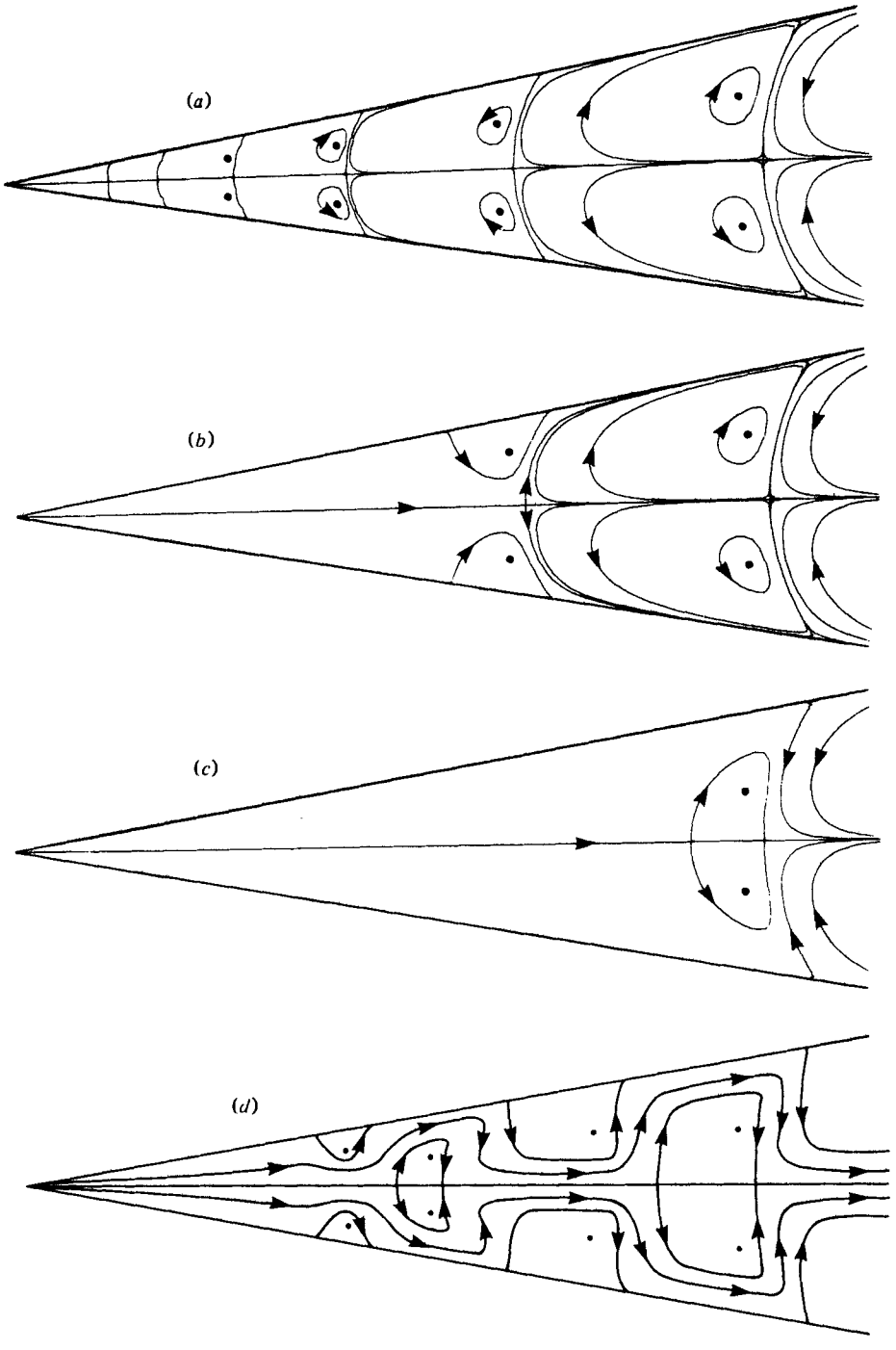

FIGURE 8. Symmetric corner eddies and source flow for $\alpha = \frac{1}{18}\pi$ and $\nu = 7{\cdot}500 + 2{\cdot}748i$. (*a*) $Q = 0$, (*b*) $Q = 50$, (*c*) $Q = 2{\cdot}5 \times 10^5$. (*d*) Schematic picture of flow.

finite size of the corner, and where there is a transition to the outer flow. Consequently, a finite number of eddies form between a minimum and a maximum distance from the gap. When the source becomes too strong, the minimum distance coincides with the maximum one and no eddies at all are formed.

The path just followed in our study of the results of Davis & O'Neill (1977) can be retraced for the work of Dorrepaal & O'Neill (1979). The important difference for the interpretation of Dorrepaal & O'Neill's work is the symmetry of their problem: both their corner region and their outer flow are symmetric about the perpendicular bisector of the line joining the centres of the cylinders. Consequently, our starting point must be the case of symmetric eddies in a corner, to which we add once again the flow produced by a line source at the vertex of the corner. The stream function is

$$\psi = r^{\nu}[\sin\nu\theta\sin(\nu-2)\alpha - \sin(\nu-2)\theta\sin\nu\alpha] + Q\frac{2\theta\cos 2\alpha - \sin 2\theta}{2\alpha\cos 2\alpha - \sin 2\alpha}. \tag{4.3}$$

The streamline patterns corresponding to two different values of Q are shown in figure 8(*b*) and (*c*). The pattern now alternates between a pair of eddies projecting from either wall and a pair of free eddies in the centre of the flow, as shown in figure 8(*d*), where distorted scales are used to clarify the pattern. It is worth noting that the free eddies contain centre stagnation points within them (marked by dots) and saddle points on their bounding streamline (where it meets the centre-line).

So far we have used existing complete solutions as inspirations for our local corner analyses. We wish now to reverse this process and synthesize a corner flow with a view to inspiring a new complete problem in Stokes flow. Having posed such a problem we shall investigate it in the next section. The corner flow we choose is one studied by Taylor (1962). The flow is produced by one wall sliding parallel to itself at speed V. The stream function for this flow, combined with antisymmetric eddies, is

$$\psi = r^{\lambda}[\cos\lambda\theta\cos(\lambda-2)\alpha - \cos(\lambda-2)\theta\cos\lambda\alpha] + Vr\left[\frac{\alpha\sin\alpha\cos\theta - \theta\sin\theta\cos\alpha}{2\alpha+\sin 2\alpha} - \frac{\alpha\cos\alpha\sin\theta - \theta\cos\theta\sin\alpha}{2\alpha-\sin 2\alpha}\right]. \tag{4.4}$$

Streamlines, as plotted by a computer, are shown in figure 9(*a*), while the overall pattern is shown schematically in figure 9(*b*). It is of incidental interest that, as V increases, the eddy attached to the wall disappears before the free eddy does, even though the free eddy is closer to the vertex of the corner. In the next section, we find a complete Stokes flow which contains similar patterns.

5. Shear flow over a cylinder touching a moving wall

If a stationary cylinder touches a moving plane wall, the corner region between them is a candidate for displaying the patterns predicted in figure 9. The stream function was given by Schubert (1967), who showed that there were no eddies in the flow. The reason for this is that the streamlines are determined by the geometry of the flow domain and not the speed of the wall V, and it happens that, in the corner, the locally forced flow is so strong compared with the eddy flow that it prevents eddies forming. If we wish to observe eddies we must increase the strength of the outer, stirring, flow. Possible ways to do this are to alter the geometry of the flow domain or to add to the

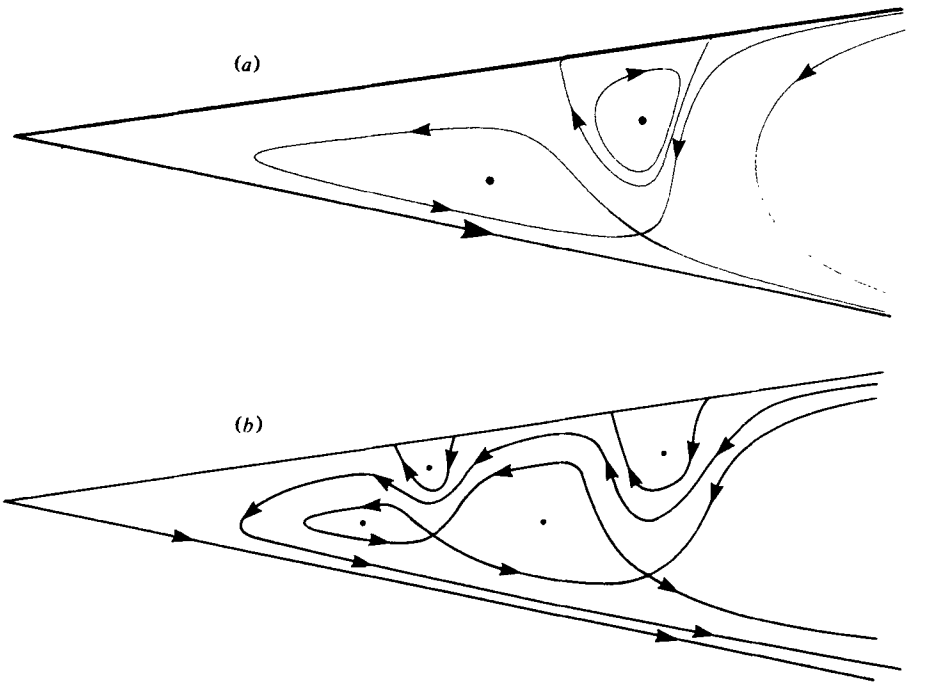

FIGURE 9. Antisymmetric eddies and flow produced by sliding wall. (*a*) $V = 3 \times 10^4$, (*b*) Schematic picture of flow. Note that successive free eddies meet at a saddle stagnation point.

moving-wall flow another flow which has a stirring component, but no locally forced component, in the corner. We can realize the latter possibility using the stream function for shear flow over a stationary cylinder and plane which was also given by Schubert (1967).

We take Cartesian co-ordinates (x, y) such that $y = 0$ is the plane of the moving wall, and define tangent-circle co-ordinates (ξ, η) by

$$\xi = y/(x^2+y^2) \quad \text{and} \quad \eta = x/(x^2+y^2).$$

The surface of the cylinder, which has unit diameter, is given by $\xi = 1$. If the shear flow has strength κ and the wall has velocity V, the stream function for the combined flow is (Schubert 1967; Davis & O'Neill 1977)

$$\psi = V\frac{\xi(\xi-1)^2}{\xi^2+\eta^2} + \tfrac{1}{2}\kappa\frac{\xi^2}{(\xi^2+\eta^2)^2} - \tfrac{1}{2}\kappa(\xi^2+\eta^2)^{-1}$$
$$\times \int_0^\infty \frac{s(\sinh s\xi - s\xi\cosh s\xi) + (e^{-s}\sinh s - s + s^2)\,\xi\sinh s\xi}{\sinh^2 s - s^2}\cos s\eta\, ds. \qquad (5.1)$$

The first term is the stream function for the moving-wall flow; it is zero on $\xi = 0$ (the plane) and $\xi = 1$ (the cylinder) and at infinity it describes a uniform stream. The next term describes the undisturbed shear flow and the final integral term describes the disturbance flow produced by the cylinder.

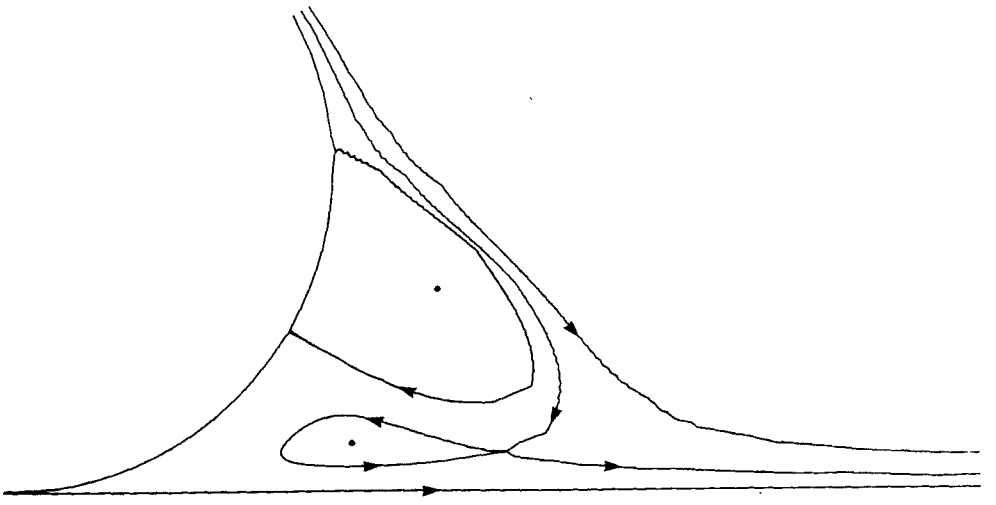

FIGURE 10. Computer plot of shear flow over a cylinder touching a moving wall for $\kappa/V = 200$.

In the region between the cylinder and the plane, where $\eta \gg 1$, the amount of computation can be reduced by using an alternative form for (5.1):

$$\psi = V\frac{\xi(\xi-1)^2}{\xi^2+\eta^2} - \tfrac{1}{2}\kappa\pi(\xi^2+\eta^2)^{-1}\,\mathrm{Re}\sum_{n=1}^{\infty}\left\{\frac{(1-\xi)\sin\lambda_n\xi + \xi\sin\lambda_n(1-\xi)}{1+\cos\lambda_n}\exp(-\lambda_n\eta)\right.$$
$$\left. - \frac{(1-\xi)\sin\mu_n\xi - \xi\sin\mu_n(1-\xi)}{1-\cos\mu_n}\exp(-\mu_n\eta)\right\}, \qquad (5.2)$$

where λ_n and μ_n are tabulated zeros of $\sin z \pm z$ (Schubert 1967; Davis & O'Neill 1977). We use a two-term approximation to (5.2) and a computer graphics package to plot the eddy motion in the corner, but the overall flow pattern is more easily deduced using the methods of §§ 2 and 3.

When V and κ are both positive, the velocity at large distances from the cylinder increases monotonically away from the plane and the flow is not too complicated. When κ/V is zero there are no eddies in the flow and so the ratio of stirring flow to local flow is increased until $\kappa/V = 31$, when the first eddy appears in the corner attached to the cylinder. A free eddy appears in the flow when $\kappa/V = 181$. In figure 10, the streamlines are shown for $\kappa/V = 200{\cdot}0$; their pattern is similar to that of figure 9(*b*). In figure 10, the wall eddy appeared before the free eddy, which is the only obvious qualitative change from figure 9. The flow outside the corner shows no unusual features.

The case in which V and κ have different signs is more complicated and displays all the types of flow discussed in § 2. The undisturbed flow is described by the stream function $\psi = Vy + \frac{1}{2}\kappa y^2$. The zero-velocity streamline is at $y = -V/\kappa$, and at that height $\psi = -\frac{1}{2}V^2/\kappa$. Above this there is a $\psi = 0$ streamline at $y = -2V/\kappa$, i.e. the volume fluxes of fluid flowing to left and right below this height are equal. These streamlines are convenient ones to refer to when describing the flow in the presence of the cylinder. We shall follow the changes in the flow pattern as the ratio $|\kappa/V|$ increases from zero. For definiteness we shall say that κ is positive and V negative.

5.1. *Weak shear flow*, $0 < -\kappa/V \ll 1$

The undisturbed zero-velocity streamline would be well above the cylinder, but it disappears in the presence of the cylinder however small κ/V is, the flow possessing instead a region of blocked fluid. To obtain more information about the flow, we expand (5.1) using κ/V as a small parameter. Thus we can show that there is a saddle stagnation point on the y axis ($\eta = 0$) at

$$y = \xi^{-1} = -V/\kappa + O(\kappa/V),$$

and at this point the stream function has the value

$$\psi = -\frac{1}{2}\frac{V^2}{\kappa}(1 + 4\kappa/V + O(\kappa^2/V^2)).$$

Since $V < 0$, we see that $|\psi|$ is less than $\frac{1}{2}V^2/\kappa$, which means that not all the fluid flowing towards the cylinder passes over it. Far from the cylinder, when $x^2+y^2 \gg 1$, the asymptotic form of ψ is

$$\psi = Vy + \tfrac{1}{2}\kappa y^2 - 2(V + A\kappa)\, y^2/(x^2+y^2) + O((x^2+y^2)^{-1}), \tag{5.3}$$

where

$$A = \frac{1}{4}\int_0^\infty \frac{s(e^{-s}\sinh s - s + s^2)}{\sinh^2 s - s^2}\, ds = 0{\cdot}72.$$

The streamlines emanating from the stagnation-point asymptote to

$$y = -V/\kappa \pm 2(-V/\kappa)^{\frac{1}{2}}.$$

The region of blocked flow is of the figure 3(c) type and without further calculation we can sketch figure 11(a) for the flow pattern. The relative dimensions in the sketch are based on $-\kappa/V = 0{\cdot}05$.

As $-\kappa/V$ increases in value, the region of blocked fluid increases in size. In addition the $\psi = 0$ streamline comes closer to the cylinder, with the result that less fluid passes the cylinder and most of it is turned back. Eventually the $\psi = 0$ streamline touches the cylinder and all the fluid approaching the cylinder along the wall is turned back. We can calculate this critical value of κ/V as follows.

5.2. *Critical value of* κ/V *when* $\psi = 0$ *streamline touches the cylinder*

The $\psi = 0$ streamline will by symmetry meet the cylinder at $x = 0$ and when this happens we shall have a point of zero tangential stress. The top of the cylinder is $\xi = 1$, $\eta = 0$ and so we calculate $\partial^2\psi/\partial\xi^2$ at this point and find the value of V/κ for which this equals zero. The result is

$$\frac{V}{\kappa} = -\frac{1}{2}\int_0^\infty \frac{s\cosh s - \sinh s}{\sinh^2 s - s^2}\, s\, ds = -1{\cdot}998,$$

i.e. $\kappa/V = -0{\cdot}5005$. The streamlines are sketched in figure 11 (b), where it can be seen that the flow at the top of the cylinder is an example of figure 2 (b) in the special case $\beta = \gamma = \frac{1}{3}\pi$.

As the value of $-\kappa/V$ is increased further the $\psi = 0$ streamline breaks, and its two halves spring from points lower down on the cylinder. The next critical value of $-\kappa/V$ we reach is the one at which the region of blocked fluid changes from being a flow like figure 3(c) to being one like figure 3(d).

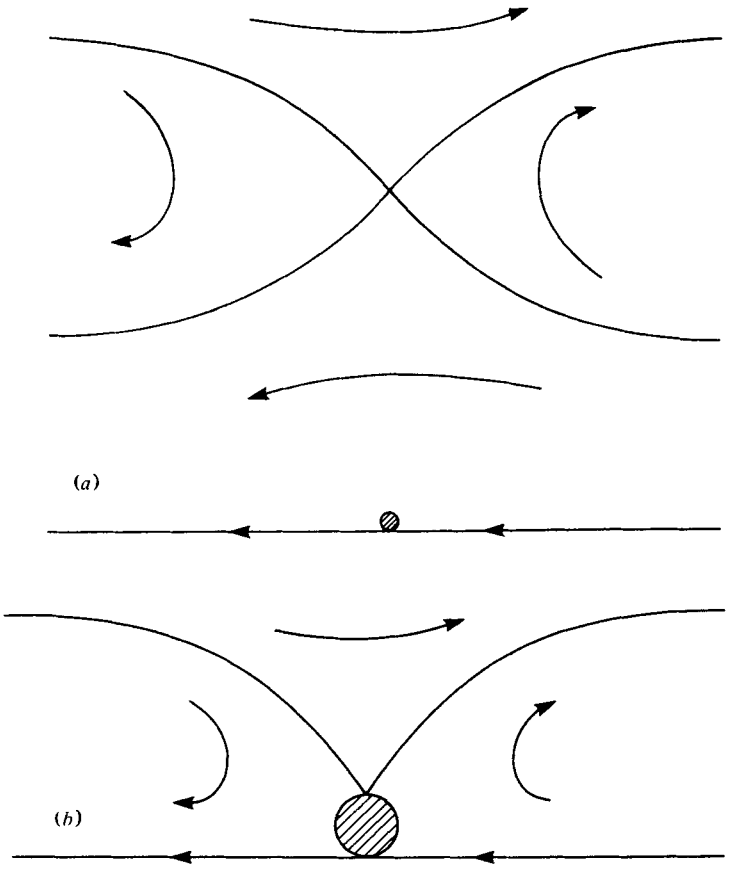

FIGURE 11 (a, b). For legend see p. 333.

5.3. *Critical value of κ/V when closed streamlines appear*

The method for establishing the change-over from flow like figure 3 (c) to that like figure 3 (d) uses the asymptotic form (5.3). We fix x at some large (positive) value x_0 and then find where $\partial\psi/\partial y$ is zero. This is the point where a streamline touches the line $x = x_0$ without crossing it. The velocity in the y direction, $\partial\psi/\partial x$, is positive at this point when the flow is like figure 3 (c) (for the choice $V < 0, \kappa > 0, x_0 > 0$) and negative when it is like figure 3 (d). In fact,

$$\partial\psi/\partial x = -4V(1+A\kappa/V)xy^2/(x^2+y^2)^2 + O(x^{-2}),$$

which has the same sign for all y, so we have immediately that the critical value is

$$\kappa/V = -A^{-1} = -1{\cdot}40.$$

There are still no eddies in the flow, however, and we must increase κ/V further to create them.

5.4. *The appearance of eddies*

An eddy appears on the cylinder after $-\kappa/V = 12000$ and a free eddy after $-\kappa/V = 17700$. In figure 11 (c), the streamlines for $-\kappa/V = 33333$ are shown as plotted by a computer. Note that far from the cylinder the asymptotic behaviour of

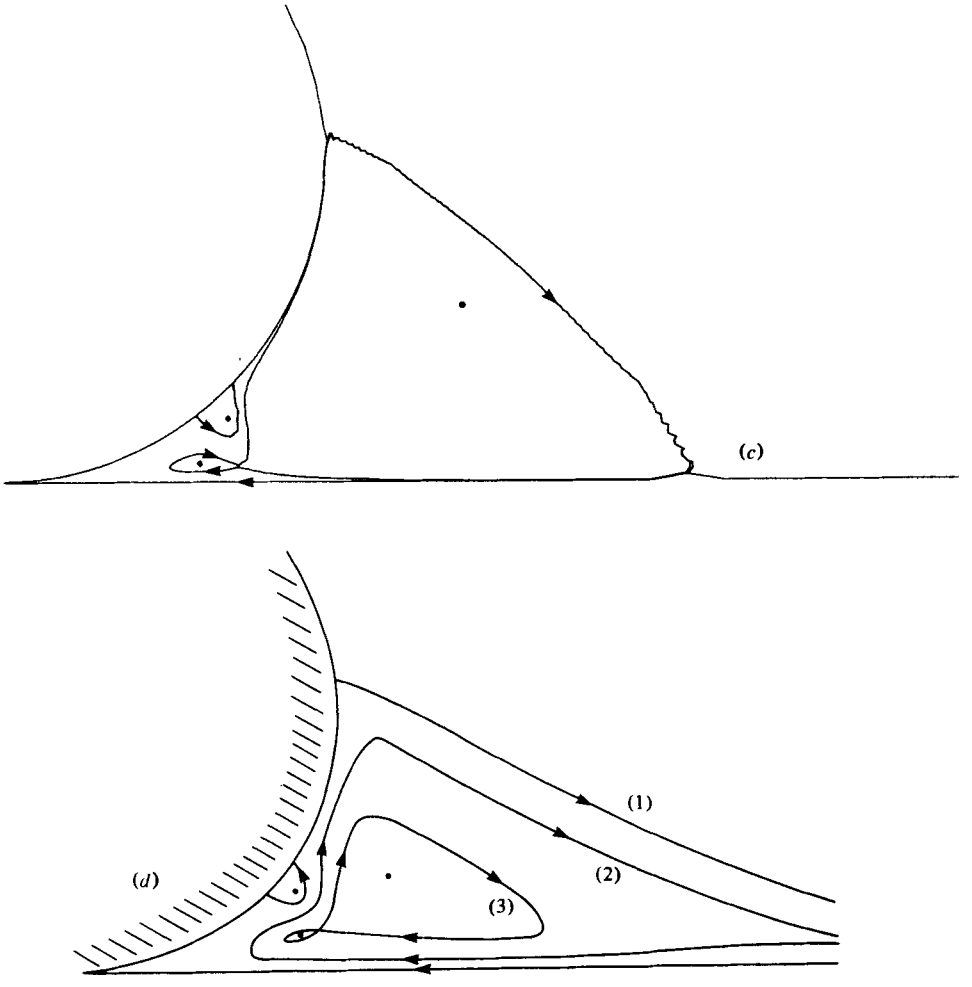

FIGURE 11. Shear flow over a cylinder touching a moving wall. (*a*) Sketch for $-\kappa/V = 0{\cdot}05$. (*b*) Sketch for $-\kappa/V = 0{\cdot}5005$. (*c*) Computer plot for $-\kappa/V = 33333$. (*d*) Schematic picture of flow for $-\kappa/V = 33333$. The scales are distorted. The labelled streamlines are (1) $\psi = 0$; (2) $\psi = -\frac{1}{2}V^2/\kappa = -4{\cdot}5 \times 10^{-10}$, boundary of closed-streamline region; (3) $\psi = -3{\cdot}1 \times 10^{-7}$, boundary of eddy. The numerical values of ψ were obtained by setting $\kappa = 1$.

the region of closed streamlines has not been resolved. The centre stagnation points have been marked by dots; the saddle point which marks the join between the free eddy and the large region of closed streamlines does not need to be identified separately. A schematic picture of the total flow is given in figure 11(*d*). When deducing this picture, we must realize that the streamline that bounds the region of closed streamlines is different from the streamline that bounds the free eddy. The stream function takes a value $-\frac{1}{2}V^2/\kappa$ on the former streamline, while on the latter it takes a value that must be determined numerically by finding the saddle stagnation point.

We wish to acknowledge the many helpful suggestions made by Professor G. K. Batchelor during this work and also the stimulating discussions held with Dr M. E. O'Neill.

REFERENCES

ADEROGBA, K. & BLAKE, J. R. 1978 *Bull. Aust. Math. Soc.* **19**, 309.

BATCHELOR, G. K. 1967 *An Introduction to Fluid Dynamics*. Cambridge University Press.

BENTWICH, M. & ELATA, C. 1965 *Phys. Fluids* **8**, 2204.

BLAKE, J. R. 1971 *Proc. Camb. Phil. Soc.* **70**, 303.

BRETHERTON, F. B. 1962 *J. Fluid Mech.* **12**, 591.

BURKILL, J. C. 1962 *A First Course in Mathematical Analysis*. Cambridge University Press.

COX, R. G., ZIA, I. Y. Z. & MASON, S. G. 1968 *J. Coll. Interface Sci.* **27**, 7.

DANDAPAT, B. S. & GUPTA, A. S. 1978 *A.I.A.A. J.* **16**, 849.

DAVIS, A. M. J. & O'NEILL, M. E. 1977 *J. Fluid Mech.* **81**, 551.

DAVIS, A. M. J., O'NEILL, M. E., DORREPAAL, J. M. & RANGER, K. B. 1976 *J. Fluid Mech.* **77**, 625.

DEAN, W. R. 1944 *Proc. Camb. Phil. Soc.* **40**, 214.

DEAN, W. R. & MONTAGNON, P. E. 1949 *Proc. Camb. Phil. Soc.* **45**, 389.

DORREPAAL, J. M. & O'NEILL, M. E. 1979 *Quart. J. Mech. Appl. Math.* **32**, 95.

HYNES, T. P. 1978 Stability of thin films. Ph.D. dissertation, Cambridge University.

LIGHTHILL, M. J. 1978 *Waves in Fluids*. Cambridge University Press.

LIRON, N. 1978 *J. Fluid Mech.* **86**, 705.

LIU, C. H. & JOSEPH, D. D. 1977 *J. Fluid Mech.* **80**, 443.

LIU, C. H. & JOSEPH, D. D. 1978 *S.I.A.M. J. Appl. Math.* **24**, 286.

LORENTZ, H. A. 1896 *Zittingsverlag Akad. v. Wert.* **5**, 168.

LUGT, H. J. & SCHWIDERSKI, E. W. 1965 *Proc. Roy. Soc. Lond.* A **285**, 382.

MARTIN, B. 1969 Numerical Studies of steady-state extrusion processes Ph.D. dissertation. Cambridge University.

MICHAEL, D. H. & O'NEILL, M. E. 1977 *J. Fluid Mech.* **80**, 785.

MOFFATT, H. K. 1964*a* *J. Fluid Mech.* **18**, 1.

MOFFATT, H. K. 1964*b* *Arch. Mech. Stosowanej* **16**, 365.

MOFFATT, H. K. & DUFFY, B. R. 1980 *J. Fluid Mech.* **96**, 299.

NIR, A. & ACRIVOS, A. 1976 *J. Fluid Mech.* **78**, 33.

PAN, F. & ACRIVOS, A. 1967 *J. Fluid Mech.* **28**, 643.

ROBERTSON, C. R. & ACRIVOS, A. 1970 *J. Fluid Mech.* **40**, 685.

SCHUBERT, G. 1967 *J. Fluid Mech.* **27**, 647.

SCHUBERT, G. 1968 *A.I.A.A. J.* **6**, 549.

SCHWIDERSKI, E. W., LUGT, H. J. & UGINCIUS, P. 1966 *J. Soc. Indust. Appl. Math.* **14**, 191.

STIMSON, M. & JEFFERY, G. B. 1926 *Proc. Roy. Soc. Lond.* A **111**, 110.

TAYLOR, G. I. 1962 *Scientific Papers*, vol. 4, pp. 410–13. Cambridge University Press 1971.

VAN DYKE, M. 1975 *Perturbation Methods in Fluid Mechanics*. Palo Alto: Parabolic Press.

WAKIYA, S. 1976 *J. Fluid Mech.* **78**, 737.

WANNIER, G. H. 1950 *Quart. Appl. Math.* **8**, 7.